Aspects of nonideal Stern–Gerlach experiment and testable ramifications

2007 J. Phys. A: Math. Theor. 40 13975

(http://iopscience.iop.org/1751-8121/40/46/010)

IOP Publishing Journal of Physics A: Mathematical and Theoretical

J. Phys. A: Math. Theor. **40** (2007) 13975–13988 doi:10.1088/1751-8113/40/46/010

Aspects of nonideal Stern–Gerlach experiment and testable ramifications

Dipankar Home[1], **Alok Kumar Pan**[1], **Md Manirul Ali**[2] **and A S Majumdar**[3]

[1] Department of Physics, Bose Institute, Calcutta 700 009, India
[2] Institute of Mathematical Sciences, C.I.T. Campus, Taramani, Chennai 600 113, India
[3] SN Bose National Centre for Basic Sciences, Block JD, Sector III, Salt Lake, Calcutta 700 098, India

E-mail: dhome@bosemain.boseinst.ac.in, apan@bosemain.boseinst.ac.in, manirul@imsc.res.in and archan@bose.res.in

Received 23 May 2007, in final form 5 September 2007
Published 31 October 2007
Online at stacks.iop.org/JPhysA/40/13975

Abstract

We critically examine the quantum-mechanical modelling of a measurement process using the Stern–Gerlach (SG) setup in the most general context, probing in particular for nonideal situations, the subtleties involved in the connection between the notion of 'distinguishability' of apparatus states defined in terms of the inner product and the spatial separation among the wave packets emerging from the SG setup. The quantitative studies highlighting some of the unexplored features of this relationship are presented in terms of an appropriately defined measure for the spatial separation between the emerging wave packets. It is also indicated how the effects arising from such departures from the idealness can be empirically tested for different values of the relevant parameters.

PACS number: 03.65.Ta

(Some figures in this article are in colour only in the electronic version)

1. Introduction

It is an inéluctable feature of the quantum measurement theory that any measurement described by the quantum mechanics entails an interaction between the measuring apparatus and the observed system resulting in the state of the measured system to be necessarily entangled with the state of the observing apparatus. The quantum-mechanical modelling for the measurement process was first introduced by von Neumann [1], where the measuring device was treated quantum mechanically; this is in contrast to Bohr's dictum [2] that a measuring device must be treated classically.

The essential theory of the quantum measurement is as follows. Let the initial state of a system be given by

$$\phi_0 = a\chi_+ + b\chi_- \tag{1}$$

where χ_+ and χ_- are the mutually orthogonal eigenstates of a measured dynamical variable. The initial combined state of the observed system and the apparatus is $\Psi_i = \phi_0\psi_0$, where ψ_0 is the initial apparatus state which is usually sharply peaked around the centre of mass of position coordinates. After the interaction with the measuring device, the final state is an entangled state which can be written as

$$\Psi_f = a\psi_+ \otimes \chi_+ + b\psi_- \otimes \chi_- \tag{2}$$

where ψ_+ and ψ_- are the apparatus states after the interaction. Thus at the end of a typical measurement interaction, there is a one-to-one correspondence between the system and the apparatus states [3].

Usually in any measurement situation the apparatus states are ultimately localized in position space. Now, for an 'ideal measurement', it is required that the apparatus states ψ_+ and ψ_- need to be *mutually orthogonal* in the configuration space and *macroscopically distinct* in the position space. Macroscopic distinguishability between apparatus states is a key notion in the quantum measurement theory which calls for careful scrutiny of its various subtleties in different experimental contexts [4].

In the context of the Stern–Gerlach (SG) setup [5] employed for measuring the spin of a quantum particle, considered to be an archetypal example of the quantum measurement, the apparatus states are represented by the spatial wavefunctions of the particles whose spins are inferred from the observed positions. While the orthogonality between the states in the configuration space does not necessarily imply the distinguishability in the position space, here in this paper we critically examine the subtleties involved in the connection between the notion of 'distinguishability' of apparatus states defined in terms of the configuration space inner product and the position space separability of the wave packets emerging from the SG magnet. In particular, we show that in any given setup the position space overlap between the emerging wave packets, defined in terms of a suitable measure, saturates to a definite time-independent value in the asymptotic limit, corresponding to any given value of the inner product, zero or otherwise. The way this saturation value varies with the relevant parameters is studied in terms of numerical estimates. Using this approach we also make a quantitative study of the departure from the idealness that can be tested experimentally.

As mentioned earlier, usually all experiments ultimately reduce to a macroscopic detection of position (pointer reading, flash of light on a screen, etc). The SG experiment exhibits *perfect* correlation between two degrees of freedom of a single system in terms of position and spin so that the value of position *definitely* allows us to infer the value of spin. In this connection we may note that the SG interferometry has been an active area of research over the past several decades. It has attracted attention of a number of well-known contributors like Bohm [6], followed by Wigner's work [7] on the problem of reconstructing the initial state and its relevance to the issue of wavefunction collapse in the quantum measurement. Subsequently, Englert, Schwinger and Scully [8] have analysed this issue in much depth (the well-known Humty-Dumpty problem) in a series of three papers. It has also been experimentally studied [9] how the extracted phase information from the SG interferometry experiment determines the transfer of coherence of spin to the external degree of freedom (position) giving rise to the position-spin entanglement. More investigation along this direction has been pursued by Oliveira and Caldeira [10] by using SQUID as the source of the magnetic field. Also, the usefulness of the SG experiment in probing more critically the subtleties of the relationship

between which path detection and interference has been recently revisited [11] in the context of the works by Dürr [12] and Knight [13].

Usually, the 'ideal limit' of the SG experiment is considered to be the one in which the inner product between the emerging wavefunctions is zero and the position space overlap between the emerging wave packets is negligibly small. In this paper we explore facets of deviations from this ideal limit; in particular, the interplay between the inner product and the position space overlap between the wave packets. When the wave packets from the SG magnet get separated and move along opposite directions, their position space overlap changes with time depending upon whether the separation of the wave packets is compared to or larger/smaller than the free broadening. What we study in detail are the quantitative aspects of the way position space overlap between the wave packets reaches a time-independent saturated value co-related with the inner product of the emerging wavefunctions for any given values of the relevant parameters of the SG setup (such as the magnetic field gradient, the interaction time and the initial width of the incident wave packet).

For the purpose of this paper the kind of situations we focus on may be categorized as the following two types: (a) *formally ideal* situation where the wavefunctions ψ_+ and ψ_- are orthogonal in configuration space (b) *operationally ideal* situation where the overlap between the associated wave packets of ψ_+ and ψ_- in the position space is negligibly small. In terms of these categorizations the usually defined 'ideal limit' defined of the SG experiment is the situation which is both formally and operationally ideal and nonideality arises whenever the required condition in either of these two situations is violated. By defining an appropriate measure for quantifying the position space separability between the wave packets emerging from the SG magnet, our scheme quantifies the departure from the usual 'ideal limit' that can be experimentally tested for nonideal situations with various ranges of values of the relevant parameters.

The discussions regarding the nonideality of the SG experiment in the literature are mostly related to the practical problem involved in ensuring the required inhomogeneity of the magnetic field [14, 15]. However, the nonideality probed here in quantitative terms arising due to a non-negligible overlap between the emergent wave packets in the position space not only pertains to the aspects not much explored but can also in practice be of significant interest in estimating the error in the inference of the value of the spin of a particle from its position on the screen placed even at large distances. Thus, our study goes through a route which is completely different from the previous authors [14, 15] who have studied the issue of nonidealness in the context of *how* to idealize the experiment. On the other hand, our present scheme is concerned with predicting verifiable outcomes in the different types of nonideal situations that we will describe in detail.

The plan of this paper is as follows. In section 2, we present a comprehensive analysis of the measurement of the spin of spin-1/2 particles using the SG setup, which has not received enough in-depth attention in the literature. In this process, we define precisely the above-mentioned notions of formal and operational idealness. This sets the stage for formulating our scheme for quantifying the departures from idealness which we study in section 3. We identify two distinct categories of operational and formal nonidealness. The actual computations of the measures of nonidealness are done for a range of relevant experimental parameter values in section 4. We provide illustrative numerical estimates showing differences of the outcomes between the ideal and nonideal situations through which we demonstrate the lack of universal correspondence between orthogonality in the configuration space and distinguishability in the position space in the SG experiment. Subsequently, we specifically illustrate the relationship between the notion of 'distinguishability' of apparatus states defined in terms of the inner product and the spatial separation between the wave packets emerging from the

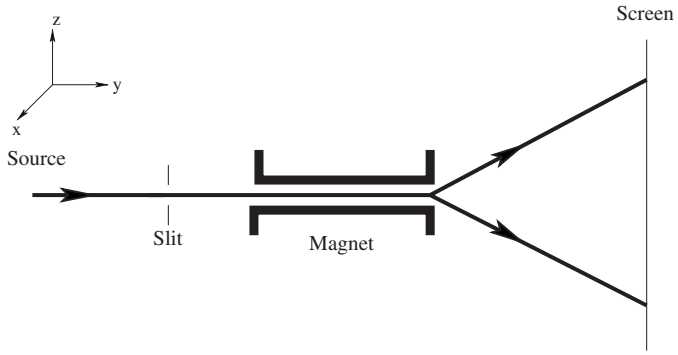

Figure 1. A schematic Stern–Gerlach setup.

SG magnet in terms of the relevant parameters. Finally, in section 5 we present our concluding remarks.

2. Quantum-mechanical treatment of SG experiment

The quantum-mechanical treatment of the SG experiment has been discussed by Bohm [6], followed by others [16]. In an interesting work, Gondran and Gondran [17] have analyzed the SG experiment using causal trajectories in the Bohmian approach. However, none of the above studies have attempted to investigate nonidealness from the present perspective. The usual description of the *ideal* SG experiment (figure 1) is as follows. A beam of *x-polarized* spin-1/2 neutral particles, say neutrons, with a finite magnetic moment is represented by the total wavefunction $\Psi(\mathbf{x}, t = 0) = \psi_0(\mathbf{x})\chi(t = 0) = \psi_0(\mathbf{x}) \otimes (\alpha|\uparrow\rangle_z + \beta|\downarrow\rangle_z)$. The spin part $\chi(t = 0)$ is the state of the system to be observed, where $|\uparrow\rangle_z$ and $|\downarrow\rangle_z$ are the eigenstates of σ_z and α and β satisfy the relation $|\alpha|^2 + |\beta|^2 = 1$. The spatial part $\psi_0(\mathbf{x})$ represents the initial state of the measuring device and is associated with a Gaussian wave packet which is initially peaked at the entry point ($\mathbf{x} = 0$) of the SG magnet and starts moving along the positive $\widehat{y}$-axis with velocity v_y through a transversely directed (along the positive $\widehat{z}$-axis) inhomogeneous magnetic field (localized between $y = 0$ and $y = d$) with respect to the direction of the beam. Within the SG magnet, in addition to the $+\widehat{y}$-axis motion the particles gain velocity with magnitude v_z along the $\widehat{z}$-axis due to the interaction of their spins with the inhomogeneous magnetic field during the time τ.

The time-evolved total wavefunction at time τ, which is an entangled state between position and spin is then given by $\Psi(\mathbf{x}, \tau) = \alpha\psi_+(\mathbf{x}, \tau) \otimes |\uparrow\rangle_z + \beta\psi_-(\mathbf{x}, \tau) \otimes |\downarrow\rangle_z$. At the exit point ($y = d$) of the SG magnet, the particles deflect differently in a way that particles with eigenstate $|\uparrow\rangle_z$ associated with the wave packet $\psi_+(\mathbf{x}, \tau)$ move freely along the direction $\widehat{n}_+ = v_y\widehat{j} + v_z\widehat{k}$ and the particles with eigenstate $|\downarrow\rangle_z$ associated with the wave packet $\psi_-(\mathbf{x}, \tau)$ move freely along the direction $\widehat{n}_- = v_y\widehat{j} - v_z\widehat{k}$. Our first task is to evaluate the explicit expressions for $\psi_+(\mathbf{x}, t)$ and $\psi_-(\mathbf{x}, t)$ corresponding to $|\uparrow\rangle_z$ and $|\downarrow\rangle_z$ after emerging from the exit point ($y = d$) of the SG magnet. To this end, we provide a fully quantum-mechanical description of the theory of the SG experiment here.

We start our calculation by taking the initial total wavefunction of the particle at $t = 0$ to be

$$\Psi(\mathbf{x}, t = 0) = \psi_0(\mathbf{x})\chi(t = 0) = \psi_0(\mathbf{x}) \otimes (\alpha|\uparrow\rangle_z + \beta|\downarrow\rangle_z) \tag{3}$$

where $\chi(t = 0) = \alpha|\uparrow\rangle_z + \beta|\downarrow\rangle_z$ is the initial spin state with $|\alpha|^2 + |\beta|^2 = 1$ and $|\uparrow\rangle_z$, $|\downarrow\rangle_z$ are the eigenstates of σ_z, and $\psi_0(\mathbf{x})$ is the initial spatial part of the total wavefunction represented

by a Gaussian wave packet which is peaked at the entry point ($\mathbf{x} = 0$) of the SG magnet at $t = 0$ given by

$$\psi_0(\mathbf{x}) = \frac{1}{\left(2\pi\sigma_0^2\right)^{3/4}} \exp\left(-\frac{\mathbf{x}^2}{4\sigma_0^2} + i\mathbf{k}.\mathbf{x}\right), \tag{4}$$

where σ_0 is the initial width of the wave packet. The wave packet moves along the positive $\widehat{y}$-axis with the initial group velocity v_y and the wave number $k_y = \frac{mv_y}{\hbar}$.

The interaction Hamiltonian is $H_{\text{int}} = \mu\boldsymbol{\sigma}.\mathbf{B}$ where μ is the magnetic moment of the neutron, $\mathbf{B}$ is the inhomogeneous magnetic field and $\boldsymbol{\sigma}$ is the Pauli spin matrices vector. Then the time-evolved total wavefunction at $t = \tau$ after the interaction of spins with the SG magnetic field is given by

$$\begin{aligned}\Psi(\mathbf{x}, t = \tau) &= \exp\left(-\frac{\mathrm{i}H\tau}{\hbar}\right)\Psi(\mathbf{x}, t = 0) \\ &= \alpha\psi_+(\mathbf{x}, \tau) \otimes |\uparrow\rangle_z + \beta\psi_-(\mathbf{x}, \tau) \otimes |\downarrow\rangle_z\end{aligned} \tag{5}$$

where $\psi_+(\mathbf{x}, \tau)$ and $\psi_-(\mathbf{x}, \tau)$ are the two components of the spinor $\psi = \binom{\psi_+}{\psi_-}$ which satisfies the Pauli equation. We take the inhomogeneous magnetic field as $\mathbf{B} = (-bx, 0, B_0 + bz)$ satisfying the Maxwell equation $\boldsymbol{\nabla}.\mathbf{B} = 0$, instead of the field chosen in the original SG paper [5] which was not divergence free. The two-component Pauli equation can then be written as two coupled equations for ψ_+ and ψ_-, given by

$$\begin{aligned}\mathrm{i}\hbar\alpha\frac{\partial\psi_+}{\partial t} &= -\alpha\frac{\hbar^2}{2m}\boldsymbol{\nabla}^2\psi_+ + \alpha\mu(B_0 + bz)\psi_+ - \beta\mu bx\psi_- \\ \mathrm{i}\hbar\beta\frac{\partial\psi_-}{\partial t} &= -\beta\frac{\hbar^2}{2m}\boldsymbol{\nabla}^2\psi_- + \alpha\mu bx\psi_+ - \beta\mu(B_0 + bz)\psi_-.\end{aligned} \tag{6}$$

Due to the realistic magnetic field, there exists an equal force transverse to the $\widehat{z}$-axis, and a continuous distribution is expected instead of the usual line distribution. But the time average of the transverse force along the $\widehat{x}$-axis is zero due to the rapid precession of the magnetic moment around the field direction [14] provided that B_0 is much greater than the degree of inhomogeneity b. By using coherent internal states, it has been argued [15] that the exact condition to neglect the tranverse component is $B_0 \gg b\sigma_0$ where σ_0 is the width of the initial wave packet. Using the above condition the coupling between the above two equations is removed and one obtains the following decoupled equations given by:

$$\begin{aligned}\mathrm{i}\hbar\frac{\partial\psi_+}{\partial t} &= -\frac{\hbar^2}{2m}\boldsymbol{\nabla}^2\psi_+ + \mu(B_0 + bz)\psi_+ \\ \mathrm{i}\hbar\frac{\partial\psi_-}{\partial t} &= -\frac{\hbar^2}{2m}\boldsymbol{\nabla}^2\psi_- - \mu(B_0 + bz)\psi_-.\end{aligned} \tag{7}$$

The solutions of the above equations can be written as

$$\begin{aligned}\psi_+(\mathbf{x}; \tau) &= \frac{1}{\left(2\pi s_\tau^2\right)^{\frac{3}{4}}}\exp\left[-\left\{\frac{x^2 + (y - v_y\tau)^2 + \left(z - \frac{v_z\tau}{2}\right)^2}{4\sigma_0 s_\tau}\right\}\right] \\ &\quad\times\exp\left[\mathrm{i}\left\{-\Delta_+ + \left(y - \frac{v_y\tau}{2}\right)k_y + k_z z\right\}\right] \\ \psi_-(\mathbf{x}; \tau) &= \frac{1}{\left(2\pi s_\tau^2\right)^{\frac{3}{4}}}\exp\left[-\left\{\frac{x^2 + (y - v_y\tau)^2 + \left(z + \frac{v_z\tau}{2}\right)^2}{4\sigma_0 s_\tau}\right\}\right] \\ &\quad\times\exp\left[\mathrm{i}\left\{-\Delta_- + \left(y - \frac{v_y\tau}{2}\right)k_y - k_z z\right\}\right],\end{aligned} \tag{8}$$

where $\Delta_{\pm} = \pm\frac{\mu B_0 \tau}{\hbar} + \frac{m^2 v_z^2 \tau^2}{6\hbar^2}$, $v_z = \frac{\mu b \tau}{m}$, $k_z = \frac{m v_z}{\hbar}$ and $s_\tau = \sigma_0\big(1 + \frac{i\hbar\tau}{2m\sigma_0^2}\big)$. The recent paper by Gondran and Gondran [17] obtains similar solutions for the two decoupled equations. They however ignore the spreading of the wave packet by taking $|s_\tau| = \sigma_0$. Moreover, the emphasis of their paper is on the description of the experiment through causal trajectories obtained by using the Bohm model and, very importantly, unlike the discussions in this paper, they do not attempt to analyse the nonidealness of the SG measurement.

Here $\psi_+(\mathbf{x}, \tau)$ and $\psi_-(\mathbf{x}, \tau)$ representing the wavefunctions at the exit point ($y = d$) of the SG magnet at $t = \tau$ correspond to $|\uparrow\rangle_z$ and $|\downarrow\rangle_z$ respectively, with average momenta $\langle\widehat{p}\rangle_\uparrow$ and $\langle\widehat{p}\rangle_\downarrow$, where $\langle\widehat{p}\rangle_{\uparrow\downarrow} = (0, mv_y, \pm\mu b\tau)$. Within the magnetic field the particles gain the same magnitude of momentum $\mu b\tau$, but the directions are such that the particles with eigenstates $|\uparrow\rangle_z$ and $|\downarrow\rangle_z$ get the drift along the positive $\widehat{z}$-axis and the negative $\widehat{z}$-axis respectively, while the $\widehat{y}$-axis momenta remain unchanged. Hence after emerging from the SG magnet the particles represented by the components $\psi_+(\mathbf{x}, \tau)$ and $\psi_-(\mathbf{x}, \tau)$ move *freely* along the respective directions $\widehat{n}_+ = v_y\widehat{j} + \frac{\mu b\tau}{m}\widehat{k}$ and $\widehat{n}_- = v_y\widehat{j} - \frac{\mu b\tau}{m}\widehat{k}$ with the *same* group velocity $v = \sqrt{v_y^2 + \big(\frac{\mu b\tau}{m}\big)^2}$ fixed by the parameters of the SG setup and the initial velocity (v_y) of the peak of the wave packet.

Now, the inner product I between the $\psi_+(\mathbf{x}, \tau)$ and $\psi_-(\mathbf{x}, \tau)$ components is given by

$$I = \int_{-\infty}^{+\infty} \psi_+^*(\mathbf{x}, \tau)\psi_-(\mathbf{x}, \tau)\, \mathrm{d}^3\mathbf{x} \tag{9}$$

and is negligibly small for the *formally ideal* situation. This inner product is preserved for the subsequent time evolution during which the freely evolving wavefunctions at any time t (here $t = 0$ is taken from $t = \tau$) *after* emerging from the SG setup are given by

$$\begin{aligned}
\psi_+(\mathbf{x}, t) &= \frac{1}{\big(2\pi s_{t+\tau}^2\big)^{3/4}} \exp\left[-\left\{\frac{x^2 + (y - v_y(\tau + t))^2 + \big(z - \frac{v_z\tau}{2} - v_z t\big)^2}{4\sigma_0 s_{t+\tau}}\right\}\right] \\
&\quad \times \exp\left[\mathrm{i}\left\{-\Delta_+ + k_y\left(y - \frac{v_y(\tau + t)}{2}\right) + k_z\left(z - \frac{v_z t}{2}\right)\right\}\right] \\
\psi_-(\mathbf{x}, t) &= \frac{1}{\big(2\pi s_{t+\tau}^2\big)^{3/4}} \exp\left[-\left\{\frac{x^2 + (y - v_y(\tau + t))^2 + \big(z + \frac{v_z\tau}{2} + v_z t\big)^2}{4\sigma_0 s_{t+\tau}}\right\}\right] \\
&\quad \times \exp\left[\mathrm{i}\left\{-\Delta_- + k_y\left(y - \frac{v_z(\tau + t)}{2}\right) - k_z\left(z + \frac{v_z t}{2}\right)\right\}\right],
\end{aligned} \tag{10}$$

where $s_{t+\tau} = \sigma_0\big(1 + \frac{i\hbar(t+\tau)}{2m\sigma_0^2}\big)$. Note that the preservation of the inner product $I = \langle\psi(\mathbf{x}, t)|\psi(\mathbf{x}, t)\rangle = \langle\psi(\mathbf{x}, \tau)|\psi(\mathbf{x}, \tau)\rangle$ for any value of t follows from the following feature. Since both the wavefunctions $\psi_+(\mathbf{x}, t)$ and $\psi_-(\mathbf{x}, t)$ freely evolve with time under the same Hamiltonian they are subjected to the same unitary operation. But the position space overlap between the two wave packets moving in opposite directions (with equal and opposite momenta of their peaks) changes with time (this aspect will be dealt with in the following section). Here the key relevant point is that the inner product is, in general, a complex quantity defined in the configuration space while the position space overlap is defined in the three-dimensional position space which is a real quantity.

Let us now discuss the outcomes of this ideal situation from the formal and operational viewpoints. In a *formally ideal* measurement $I \approx 0$. After emerging from the exit point of the SG magnet the probabilities of finding particles with up and down spins in the $\widehat{z}$-axis, i.e., $|\uparrow\rangle_z$ and $|\downarrow\rangle_z$, are $P_\uparrow^i = |\alpha|^2$ and $P_\downarrow^i = |\beta|^2$, respectively. In order to discriminate the above situation from the case of an *operationally ideal* situation, we define the *operational*

idealness by the condition that the probabilities of finding particles within the positive zy-plane (*upper* plane) and negative zy-plane (*lower* plane) are $P_+^i = |\alpha|^2$ and $P_-^i = |\beta|^2$, respectively. Combining these two statements coming from the formal and the operational viewpoints, we can say that when a measurement is *both formally and operationally ideal* then $P_+^i = P_\uparrow^i$ and $P_-^i = P_\downarrow^i$, i.e., the probability of finding $|\uparrow\rangle_z$ particles equals the probability of finding particles in the upper plane, and similarly for $|\downarrow\rangle_z$ particles and those in the lower plane. In other words, in a perfectly (formally as well as operationally) ideal SG experiment, all $|\uparrow\rangle_z$ particles can be found in the upper plane, whereas all $|\downarrow\rangle_z$ particles can be found in the lower plane.

3. The nonideal SG experiment

In the context of the SG experiment the above-discussed ideal situation is a very special case because, in general, *orthogonality* between $\psi_+(\mathbf{x}, \tau)$ and $\psi_-(\mathbf{x}, \tau)$ crucially depends on the delicate choices of some relevant parameters involved in the SG setup. Substituting the expressions for $\psi_+(\mathbf{x}, \tau)$ and $\psi_-(\mathbf{x}, \tau)$ given by equation (8) into equation (9), one obtains the actual expression for the inner product $|I|$ (the inner product may contain a global phase and hence we take the modulus of the inner product) to be

$$|I| = \exp\left\{-\frac{\mu^2 b^2 \tau^4}{8m^2\sigma_0^2} - \frac{2\mu^2 b^2 \tau^2 \sigma_0^2}{\hbar^2}\right\} \tag{11}$$

which will be preserved after subsequent free time evolution. It is seen from equation (11) that $|I|$ depends on the parameters b, τ, m and σ_0 and for *sufficiently large* values of b and τ with fixed σ_0 and m, one has $|I| \approx 0$, i.e., $\psi_+(\mathbf{x}, t)$ and $\psi_-(\mathbf{x}, t)$ are *orthogonal* for all practical purposes. But in general, as we will see in the following section, there could be various choices of the relevant parameters for which $|I| > 0$.

Our purpose here is how to explore the *nonideal* situation from the viewpoints of both formal orthogonality and operational distinguishability and investigate the connection between the two by quantifying the departures from the ideal measurement outcomes. The question arises as to how one can predict the outcomes of this nonideal experiment. It is well known that nonorthogonal states can *not* be distinguished perfectly, even if they are known. There are various schemes [18] for optimum discrimination among the states by adopting different strategies. Usually all experiments ultimately reduce to the measurement of position, and here in this work we are confined to the operational discrimination between the states in the position space.

From the operational viewpoint, the above question may be posed as follows: what is the probability of finding particles with $|\uparrow\rangle_z$ (or $|\downarrow\rangle_z$) in the *lower plane* (or *upper plane*) when $|I|$ is *not negligibly small*? In order to find an answer to this, we define an *error integral* $E(t)$, the key ingredient in our scheme which gives a quantitative prediction for this nonideal situation. The error integral $E(t)$ is a function of time and is given by

$$\begin{aligned} E(t) &= \int_{x=-\infty}^{+\infty}\int_{y=-\infty}^{+\infty}\int_{z=0}^{+\infty} |\psi_-(\mathbf{x}, t)|^2 \,\mathrm{d}x\,\mathrm{d}y\,\mathrm{d}z \\ &= \int_{x=-\infty}^{+\infty}\int_{y=-\infty}^{+\infty}\int_{z=-\infty}^{0} |\psi_+(\mathbf{x}, t)|^2 \,\mathrm{d}x\,\mathrm{d}y\,\mathrm{d}z, \end{aligned} \tag{12}$$

where $E(t)$ multiplied by $|\alpha|^2$ (or $|\beta|^2$) gives the probability of finding $|\downarrow\rangle_z$ (or $|\uparrow\rangle_z$) particles within the upper plane (or lower plane) at time t. Note that the error integral $E(t)$ is a real quantity unlike the inner product, and it changes with time as the two wave packets $|\psi_+(x, t)|^2$

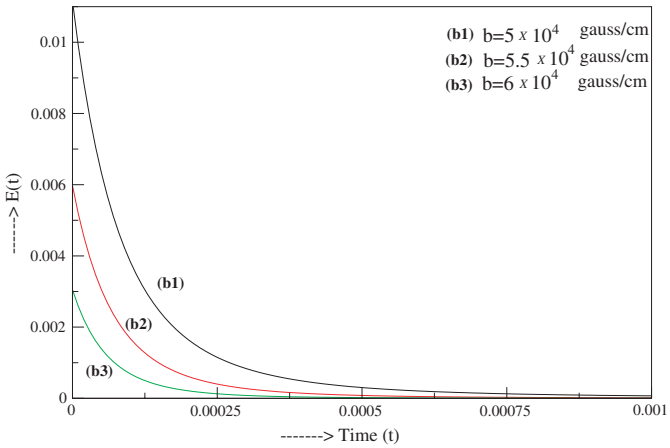

Figure 2. The variation of $E(t)$ with time (in seconds) is shown for three different values of b, i.e., $b = 5 \times 10^4$ G cm^{-1}, $b = 5.5 \times 10^4$ G cm^{-1} and $b = 6 \times 10^4$ G cm^{-1} with $\tau = 5 \times 10^{-4}$ s and $\sigma_0 = 10^{-5}$ cm while $E_s \approx 0$ and $|I| \approx 0$ [case (i)].

and $|\psi_-(x, t)|^2$ emerging from the SG setup move along opposite directions with equal and opposite momenta of their peaks. It then turns out from the solutions given by equation (10) that the parameter $E(t)$ is *not* zero just after the two wave packets emerge from the SG magnet at $t = \tau$, but during the course of a free evolution $E(t)$ saturates to a minimum value, say E_s, with the saturation time t_s depending upon the choices of relevant parameters involved. It is then logical to consider E_s as a measure of the nonidealness. The value of E_s varies between *zero* and *one-half*, depending upon the values of the relevant parameters b, τ, m and σ_0, so that $E_s \approx 0$ represents the *operationally ideal* situation, whereas $E_s = 0.5$ the *fully nonideal* one.

Note that $|I|$ is *not* the measure of operational nonidealness, but the modified observable probability is concerned with the E_s. Now, the *modified observable probabilities* of finding the particles with $|\uparrow\rangle_z$ (spin up) in the *upper plane* and $|\downarrow\rangle_z$ (spin down) in the *lower plane* under the nonideal situation are respectively given by

$$P_{\uparrow}^{\rm ni} = (1 - E_s)|\alpha|^2 \qquad P_{\downarrow}^{\rm ni} = (1 - E_s)|\beta|^2, \tag{13}$$

where $P_{\uparrow}^{\rm ni} + P_{\downarrow}^{\rm ni} \neq 1$. In this case, in the upper (or lower) plane we get a *mixture* of particles with both spin states $|\uparrow\rangle_z$ and $|\downarrow\rangle_z$. Hence the probabilities of finding $|\downarrow\rangle_z$ particles in the upper plane and $|\uparrow\rangle_z$ particles in the lower plane are $E_s|\beta|^2$ and $E_s|\alpha|^2$, respectively. Then the probabilities of finding both $|\uparrow\rangle_z$ and $|\downarrow\rangle_z$ particles the *total probability in the upper plane* and the *total probability in the lower plane* are respectively given by

$$P_{+}^{\rm ni} = (1 - E_s)|\alpha|^2 + E_s|\beta|^2 \qquad P_{-}^{\rm ni} = (1 - E_s)|\beta|^2 + E_s|\alpha|^2, \tag{14}$$

where $P_{+}^{\rm ni} + P_{-}^{\rm ni} = 1$ and $E_s = 0$ gives the result of the ideal measurement. These $P_{+}^{\rm ni}$ and $P_{-}^{\rm ni}$ constitute the basic observable probabilities in our scheme. To verify equation (14) one needs to suitably place a subsequent *usual ideal* SG setup with $|I| \approx 0$ (at a sufficiently large distance where the asymptotic condition $E_s \approx 0$ is satisfied), which counts all particles in the upper plane. Then the probabilities of finding $|\uparrow\rangle_z$ and $|\downarrow\rangle_z$ are $(1 - E_s)|\alpha|^2$ and $E_s|\beta|^2$, respectively.

As we have defined above, $|I| \approx 0$ implies the formally ideal situation, and $E_s = 0$ the operationally ideal situation. Within the context of the nonideal SG experiment, it is then

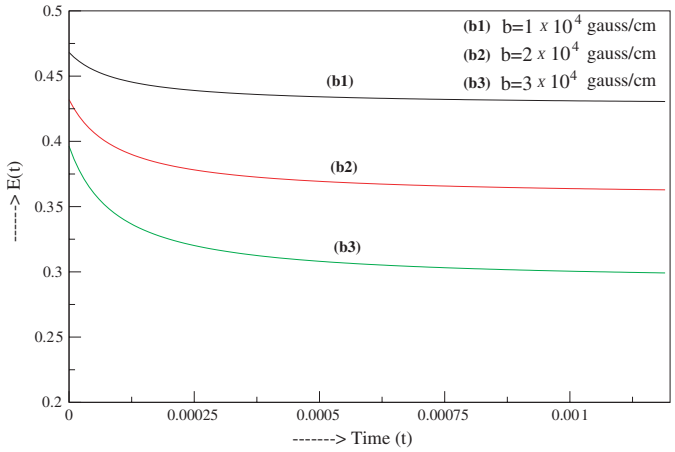

Figure 3. The variation of $E(t)$ with time (in seconds) is shown for the values $b = 1 \times 10^3$ G cm^{-1}, $b = 2 \times 10^3$ G cm^{-1} and $b = 3 \times 10^3$ G cm^{-1}, respectively, with $\tau = 10^{-4}$ s and $\sigma_0 = 10^{-4}$ cm while $E_s \gg 0$ and $|I| = 0.9323$, 0.7925 and 0.5921 for (b1), (b2) and (b3) respectively [case (ii)].

possible to identify the following distinct situations which highlight the possible connections between the configuration space orthogonality and the position space distinguishability.

(i) If the situation is *operationally ideal* ($E_s \approx 0$), then it *must be formally ideal* ($|I| \approx 0$). Or in other words, the observation of the position space distinguishability implies that the two wavefunctions are orthogonal in the configuration space.

(ii) If the situation is *formally nonideal* ($|I| > 0$), then it *must be operationally nonideal* ($E_s > 0$). This means that the vanishing of $|I|$ is a necessary condition for the 'ideal limit'. This is the usual nonideal situation which has been studied by earlier authors [14, 15] with the aim of reducing the magnitude of nonidealness.

(iii) If the situation is *formally ideal* ($|I| \approx 0$), still it *may be operationally nonideal* ($E_s > 0$). This is particularly interesting because it shows that the vanishing of $|I|$ is essentially a necessary condition for the 'ideal limit' but it is *not* sufficient condition. We probe some unexplored features of such a nonideal situation in a quantitative way; in particular, we study the link between the notion of 'distinguishability' of apparatus states defined in terms of the configuration space inner product and the position space overlap between the wave packets emerging from the SG magnet.

4. Quantitative estimates

We will now show explicitly how the different situations (i), (ii) and (iii) arise due to the choices of the parameters in the SG experiment. In order to illustrate these features, we present some numerical estimates for the probabilities $P^{\rm ni}_{\uparrow}$ and $P^{\rm ni}_{\downarrow}$, and $P^{\rm ni}_{+}$ and $P^{\rm ni}_{-}$ given in equations (13) and (14), respectively. The estimation of these probabilities is contingent on the values of α, β and E_s. We first show three representative figures (figures 2–4) corresponding to situations (i), (ii) and (iii) respectively, which indicate how the parameter $E(t)$ varies with time and saturates to E_s (which is *not* always zero). The curves in the figures are plotted by taking various choices of the relevant parameters, such as the degree of inhomogeneity of the magnetic field b, and the interaction time τ while the initial width of the Gaussian wave packet σ_0 and the mass m of the neutron are fixed.

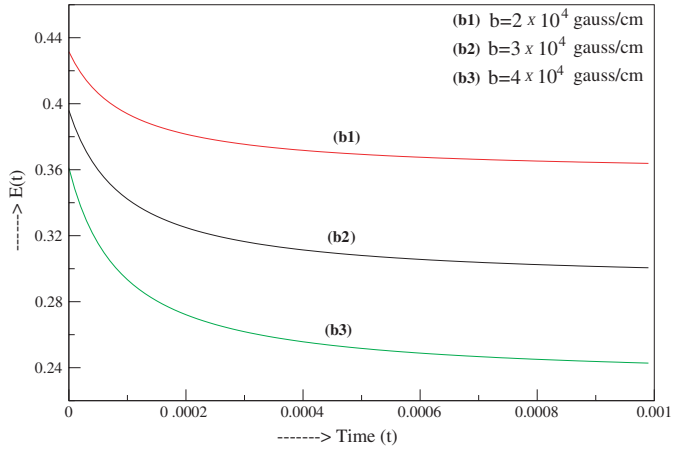

Figure 4. The variation of $E(t)$ with time (in sec) is shown for the values $b = 2 \times 10^4$ G cm^{-1}, $b = 3 \times 10^4$ G cm^{-1} and $b = 4 \times 10^4$ G cm^{-1}, respectively, with $\tau = 10^{-4}$ s and $\sigma_0 = 10^{-5}$ cm while $E_s > 0$ although $|I| \approx 0$ [case (iii)].

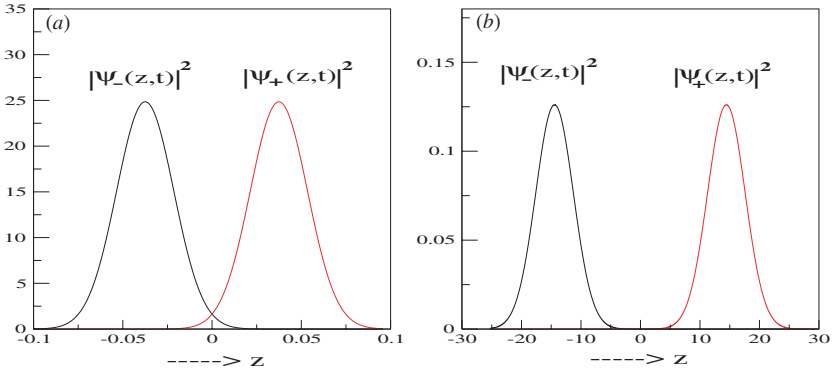

Figure 5. The overlap between $|\psi_+(z,t)|^2$ and $|\psi_-(z,t)|^2$ is plotted for $b = 6 \times 10^4$ G cm^{-1}, $\tau = 5 \times 10^{-4}$ s and $\sigma_0 = 10^{-5}$ cm at two different times (*a*) $t = 10^{-5}$ s and (*b*) $t = 0.1$ s while $|I| \approx 0$ and $E_s \approx 0$ [case (i)].

Corresponding to the above three cases, we further plot the snapshots of the overlap between $|\psi_+(z,t)|^2$ and $|\psi_-(z,t)|^2$ (figures 5–7) for three different sets (Set-I, Set-II and Set-III) of the relevant parameters τ, b and σ_0 at two different times $t = 10^{-5}$ s and $t = 0.1$ s. For Set-I, $b = 6 \times 10^4$ G cm^{-1}, $\tau = 5 \times 10^{-4}$ s and $\sigma_0 = 10^{-5}$ cm. For Set-II, $b = 2 \times 10^3$ G cm^{-1}, $\tau = 10^{-4}$ s and $\sigma_0 = 10^{-4}$ cm. For Set-III, $b = 4 \times 10^4$ G cm^{-1}, $\tau = 10^{-4}$ s and $\sigma_0 = 10^{-5}$ cm. These Set-I, Set-II and Set-III correspond to the three situations (i), (ii) and (iii) respectively as discussed earlier. One can see from figure 7 that there exists a finite and appreciable overlap between $|\psi_+(\mathbf{x},t)|^2$ and $|\psi_-(\mathbf{x},t)|^2$ at $t = 10^{-5}$ s which does *not always* vanish at $t = 0.1$ s (which is much larger than the saturation time t_s), although the inner product is negligibly small, i.e., $|I| < 10^{-100}$.

We now use the parameters of Set-III to calculate the probabilities for finding spin-up $P^{\rm ni}_{\uparrow}$ and spin-down $P^{\rm ni}_{\downarrow}$ particles from equation (13) in the formally ideal but operationally nonideal situation [case (iii)] and the corresponding probabilities $P^{\rm ni}_{+}$ and $P^{\rm ni}_{-}$ in the upper and

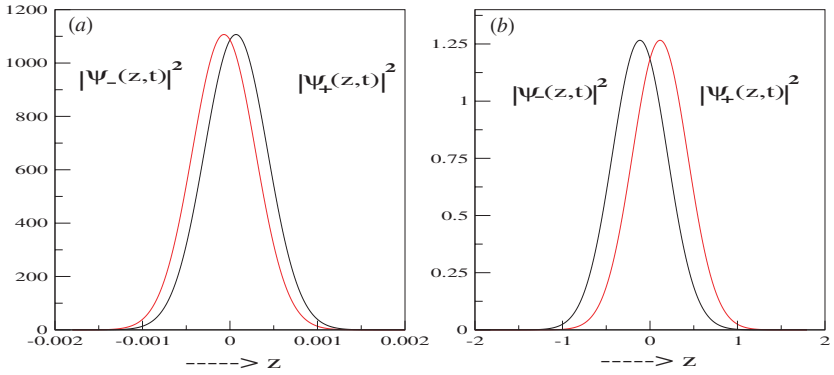

Figure 6. The overlap between $|\psi_+(z,t)|^2$ and $|\psi_-(z,t)|^2$ is plotted for $b = 2 \times 10^3$ G cm^{-1}, $\tau = 10^{-4}$ s and $\sigma_0 = 10^{-4}$ cm at two different times (*a*) $t = 10^{-5}$ s, and (*b*) $t = 0.1$ s while $|I| > 0$ and $E_s > 0$ [case (ii)].

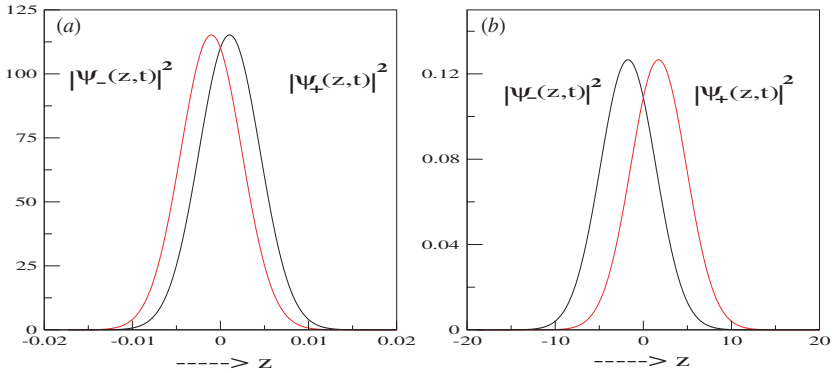

Figure 7. The overlap between $|\psi_+(z,t)|^2$ and $|\psi_-(z,t)|^2$ is plotted for $b = 4 \times 10^4$ G cm^{-1}, $\tau = 10^{-4}$ s and $\sigma_0 = 10^{-5}$ cm at two different times (*a*) $t = 10^{-5}$ s and (*b*) $t = 0.1$ s while $|I| \approx 0$ but $E_s > 0$ [case (iii)].

lower planes, respectively from equation (14). We choose four different values for α and β satisfying $|\alpha|^2 + |\beta|^2 = 1$. The saturation value of E_t is obtained to be $E_s = 0.2478$. The results are presented in table 1.

It is seen from table 1 that when $\alpha = \beta = 1/\sqrt{2}$ the probability of finding particles with *both* $|\uparrow\rangle_z$ and $|\downarrow\rangle_z$ spins *in the upper plane* is $P_+^{\rm ni} = 0.5000$, where the probability of finding $|\uparrow\rangle_z$ (and $|\downarrow\rangle_z$) *in the upper plane* is $P_\uparrow^{\rm ni} = 0.3761$ (and $P_\downarrow^{ni} = 0.1239$). Note that in the usual ideal situation (i) the probability of finding particles with $|\uparrow\rangle_z$ in the upper plane is $P_+^i = P_\uparrow^i = 0.5000$. To test the result experimentally, a subsequent SG setup which is *ideal* in the sense of our situation (i), i.e., $|I| \approx 0$ and $E_s \approx 0$, needs to be suitably placed. The purpose of the first SG magnet is to separate nonideally the two packets, but there is no detection of particles involved at this stage. The position of the second SG setup as well as the screen position must be beyond the corresponding saturation position $Y_s = v_y t_s$. The value of t_s and subsequently E_s is different for different parameter choices. For the parameters chosen in table 1, $t_s = 0.0012$ s and hence the possible position of the second SG setup Y_s is beyond 12 cm if one takes $v_y = 10^4$ cm s^{-1}.

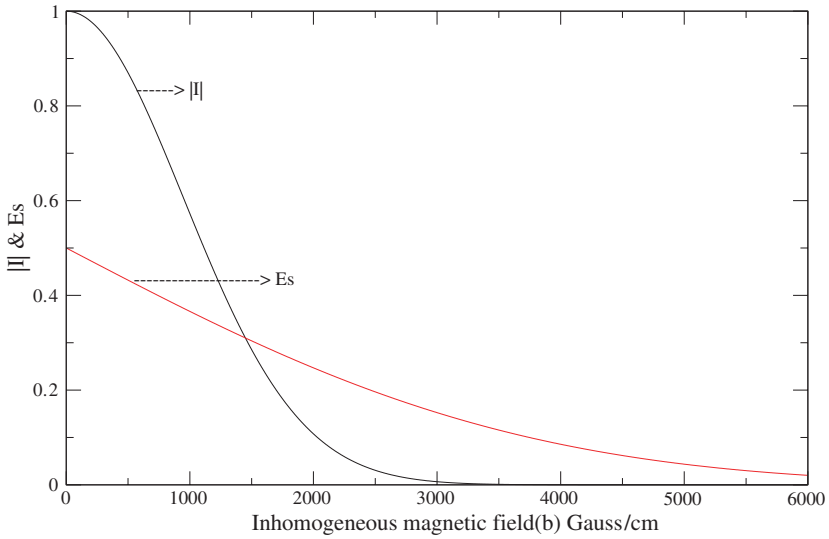

Figure 8. The variation of the inner product ($|I|$) and the saturated value of the error integral (E_s) with respect to the inhomogeneous magnetic field (b) are shown for $\sigma_0 = 10^{-4}$ cm and $\tau = 3 \times 10^{-4}$ s. The maximum values of $|I|$ and E_s are 1 and 0.5 respectively when $b = 0$. Note that, $|I|$ decreases towards zero more rapidly than E_s for increasing b.

Table 1. The quantities $P^i_\uparrow$ and $P^i_\downarrow$ denote the observable probabilities for finding respectively, the spin-up and spin-down particles corresponding to $|\uparrow\rangle_z$ and $|\downarrow\rangle_z$ of the *ideal* SG measurement and $P^{ni}_\uparrow$ and $P^{ni}_\downarrow$ are the same for the *nonideal* case. The quantities P^i_+ and P^i_- denote the observable probabilities of finding particles *in the upper plane* and *in the lower plane* of the *ideal* SG measurement and P^{ni}_+ and P^{ni}_- are the same for the *nonideal* case. Note that $P^i_\uparrow = P^i_+$ and $P^i_\downarrow = P^i_-$. In this table the results are presented for four different choices of α and β satisfying $|\alpha|^2 + |\beta|^2 = 1$ with $E_s = 0.2478$ for the relevant parameters $b = 4 \times 10^4$ G cm^{-1}, $\tau = 10^{-4}$ s and $\sigma_0 = 10^{-5}$ cm while $|I| \approx 0$ [case (iii)].

α	β	$P^i_\uparrow = P^i_+$	$P^i_\downarrow = P^i_-$	$P^{\rm ni}_\uparrow$	$P^{\rm ni}_\downarrow$	$P^{\rm ni}_+$	$P^{\rm ni}_-$
$1/\sqrt{2}$	$1/\sqrt{2}$	0.5000	0.5000	0.3761	0.3761	0.5000	0.5000
0.8000	0.6000	0.6400	0.3600	0.4814	0.2708	0.5706	0.4294
$\sqrt{3}/2$	1/2	0.7500	0.2500	0.5642	0.1881	0.6261	0.3739
0.9487	0.3162	0.9000	0.1000	0.6770	0.0752	0.7018	0.2982

Next, we probe the possible connection between the modulous of the inner product ($|I|$) and the saturated value of the error integral (E_s). In order to study this connection we plot the variation of $|I|$ and E_s with respect to the strength of the inhomogeneous magnetic field (b) where the initial width of the wave packet is $\sigma_0 = 10^{-4}$ cm and the interaction time within the SG magnet is $\tau = 3 \times 10^{-4}$ s. When $b = 0$, the values of $|I|$ and E_s are maximum, and then with the increasing b, both $|I|$ and E_s decrease but $|I|$ falls towards zero more rapidly than E_s. The value of E_s tends to zero beyond $b = 6000$ G cm^{-1}, while $|I|$ becomes negligibly small around $b = 3500$ G cm^{-1}. It may be noted that in the original SG experiment [5] the value of b was chosen to be $b \approx 10\,000$ G cm^{-1}.

Such quantitative estimates pertaining to the curves in figure 8 can be done for other types of situations such as by varying the initial width of the wave packet or the interaction

time within the SG magnet which depends upon the initial group velocity of the wave packet.

5. Conclusions

It needs to be stressed that all the quantitative estimates given in this paper are based on the measure of the position space overlap between the wave packets emerging from the SG magnet taken to be the error integral $E(t)$ given by equation (12) which is used to predict the results of the *nonideal* situations where the probabilities for finding $|\uparrow\rangle_z$ particles in the lower plane and for finding $|\downarrow\rangle_z$ particles in the upper plane are both significantly *non-vanishing*. We find that the time-independent saturation value of the error integral E_s can be non-zero for a wide range of relevant parameters such as the degree of the inhomogeneous magnetic field and the interaction time within the SG magnet. Thus, in nonideal situations, we can predict the observable outcomes, i.e., the probabilities $P_+^{\rm ni}$ and $P_-^{\rm ni}$ corresponding to both $|\uparrow\rangle_z$ and $|\downarrow\rangle_z$ particles in the upper and lower planes, respectively. These predictions can be experimentally verified by placing a screen for detecting the particles beyond the second SG setup (both formally and operationally ideal) through which those selected particles emerging from the first SG setup are passed which are confined in the upper plane ($z = 0$ to $z \to \infty$).

It is thus important to evaluate theoretically in a formally ideal $|I| \approx 0$ but operationally nonideal ($E_s > 0$) situation as to what will be the possible outcomes of the SG experiment when it is used in its various applications [6–13] mentioned in the beginning. The utility of such a scheme for quantifying the nonidealness in any given SG setup lies in enabling the estimation of error involved in inferring the measured spin state (i.e., the error in the state reconstruction process) from the actual measurement results. That this situation may arise even in the formally ideal case with operational nonidealness adds further interest to the estimation of such observable outcomes.

It should, therefore, be instructive to pursue such quantitative studies in terms of other ways of defining the position space separation between the wave packets emerging from the SG setup. For example, one may use the von Neumann criterion [1] for defining such separability in terms of the separation between the peaks of the emerging wave packets and their respective width at any instant t. In particular, the nature of the connection between the notion of 'distinguishability' of apparatus states defined in terms of the configuration space inner product and the spatial separation between the wave packets emerging from the SG magnet shown in the figure 8 will be critically dependent on *how* the *position space separability* is defined.

Furthermore, the analysis of the operational nonidealness is likely to have quantitative implications in the SG interferometry. For example, one can attempt a nonideal variant of an interesting example of quantum-state reconstruction [19] involving the analysis of a synthesis of noncommuting observables of spin-1/2 particles using the SG device with varying orientations. As indicated by Hradil *et al* [19], the formalism developed for the analysis of such examples can be applied to the study of various problems such as the estimation of the quantum state inside split-beam neutron interferometers. We also note that since the effect of environment-induced decoherence on the position space overlap of the wave packets has been studied in an ideal SG setup [20], it should be interesting to investigate such effects in the types of nonideal SG setups discussed in this paper.

Finally, such quantitative studies of nonideal situations using the SG setup could be useful for gaining new insights into the quantum theory of nonideal measurement. From this perspective more studies on the quantum-mechanical modelling of nonideal variants of different types of measurement situations should be interesting.

Acknowledgments

We are grateful to John Corbett of Macquarie University, Australia for stimulating discussions. We also thank the anonymous referee for very helpful comments. DH acknowledges the support from the Centre for Science and Consciousness, Kolkata, India. AKP acknowledges the support from the Council of Scientific and Industrial Research, India.

References

[1] von Neumann J 1966 *Mathematical Foundations of Quantum Mechanics* (Princeton, NJ: Princeton University Press)
[2] Bohr N 1948 *Dialectica* **2** 312
[3] Home D 1997 *Conceptual Foundations of Quantum Physics* (New York: Plenum) chapter 2
[4] Leggett A J 2002 *J. Phys.: Condens. Matter* **14** R415
[5] Gerlach W and Stern O 1922 *Z. Phys.* **9** 349
[6] Bohm D 1952 *Quantum Theory* (Englewood Cliffs, NJ: Prentice-Hall)
[7] Wigner E P 1963 *Am. J. Phys.* **31** 6
[8] Englert B G, Schwinger J and Scully M O 1988 *Found. Phys.* **18** 1045
Scully M O, Schwinger J and Englert B G 1988 *Z. Phys.* D **10** 135
Scully M O, Englert B G and Schwinger J 1989 *Phys. Rev.* A **40** 1775
[9] Miniatura C, Robert J, Gorceix O, Lorent V, Le Boiteux S, Reinhardt J and Baudon J 1992 *Phys. Rev. Lett.* **69** 261
Robert J, Gorceix O, Lawson-Daku J, Nic Chomaric S, Miniatura C, Baudon J, Peralls F, Eminyar M and Rubin K 1995 *Fundamental Problems in Quantum Theory, Part III* ed D M Greenberger and A Zeilinger *Ann. New York Acad. Sci.* **755** 173
[10] de Oliveira T R and Caldeira A 2006 *Phys. Rev.* A **73** 042502
[11] Reinisch G 1999 *Phys. Lett.* A **259** 427
[12] Dürr S, Nonn T and Rempe G 1998 *Nature* **395** 33
[13] Knight P 1998 *Nature* **395** 12
[14] Alstrom P, Hjorth P and Muttuck R 1982 *Am. J. Phys.* **50** 697
Singh S and Sharma N K 1983 *Am. J. Phys.* **52** 274
[15] Cruz-Barrios S and Gomez-Camacho J 2000 *Phys. Rev.* A **63** 012101
Potel G, Barranco F, Cruz-Barrios S and Gómez-Camacho J 2005 *Phys. Rev.* A **71** 052106
[16] Scully M O, Lamb W E Jr and Barut A 1987 *Found. Phys.* **17** 575
Busch P and Schroeck F E 1989 *Found. Phys.* **19** 807
Platt D E 1992 *Am. J. Phys.* **60** 306
Patil S H 1998 *Eur. J. Phys.* **19** 25–30
Roston G B, Casas M, Plastino A and Plastino A R 2005 *J. Phys. A: Math. Gen.* **26** 657
[17] Gondran M and Gondran A 2005 *Preprint* quant-ph/0511276
[18] Ivanovic I D 1987 *Phys. Lett.* A **123** 257
Dieks D 1988 *Phys. Lett.* A **126** 303
Peres A 1988 *Phys Lett.* A **128** 19
Chefles A 2000 *Contemp. Phys.* **41** 401
[19] Hradil Z, Summhammer J, Badurek G and Rauch H 2000 *Phys. Rev.* A **62** 014101
[20] Venugopalan A 1997 *Phys. Rev.* A **56** 4307
Venugopalan A 2000 *Phys. Rev.* A **61** 012102